Ultrasonic Attenuation in Antimony. II. de Haas–van Alphen Oscillations*†

J. B. KETTERSON‡§
Department of Physics and Institute for the Study of Metals, University of Chicago, Chicago, Illinois
(Received 11 July, 1962)

De Haas–van Alphen oscillations in the magnetoacoustic attenuation in single crystals of antimony were measured at 1.2°K in the range of fields from 4000 to 9100 G for the field in the x-z, y-z, and x-y planes. In addition to the carriers observed by Shoenberg, new carriers are seen. Evidence of nonellipsoidal behavior of the Fermi surface of the new carriers is observed.

INTRODUCTION

ULTRASONIC sound has in recent years proved to be a powerful tool for investigating the band structure of metals and semimetals. There are three important ultrasonic effects: cyclotron resonance,[1,2] geometric resonance (GR),[2–5] and de Haas–van Alphen oscillations (dHvA).[6,7] The first occurs by resonant absorption of sound energy when the cyclotron frequency, or a submultiple of it, is equal to the sound frequency. The condition for observation is $\omega_c\tau\gg1$, where ω_c is the usual cyclotron frequency. Geometric resonance results from a variation in the interaction of the electron with the sound wave when the orbital diameter of the electron is a multiple of the sound wavelength. To observe this effect one must have $ql\gg1$, where q is the sound wave number and l the mean free path. The third effect, which is quantum mechanical, as opposed to the other two which are semiclassical, occurs when the energy separation of adjacent Landau levels is greater than kT; in addition to this condition the electron must be able to complete many orbits before being scattered which again requires $\omega_c\tau\gg1$.

Cyclotron resonance could not be observed because the relaxation times in our samples were too short for the frequencies we had available. Geometric resonance was observed and is reported by Eckstein in the preceding paper.[8] This paper reports the results of de Haas–van Alphen oscillations in antimony.

THEORY

A theory for ultrasonic dHvA oscillations has been given by Stolz.[9] His theory is not self-consistent and neglects relaxation time effects. We will assume with Onsager[10] that the period of the oscillations is given by

$$\Delta(1/H)=eh/c\mathcal{A}, \tag{1}$$

where H is the magnetic field; $\Delta(1/H)=1/H_i-1/H_{i+1}$, where i and $i+1$ are maxima or minima of successive oscillations, and $\mathcal{A}$ is the extremal cross-sectional area of the Fermi surface in momentum space perpendicular to the magnetic field. The constants e, h, and c, are, respectively, the charge of the electron, Planck's constant, and the velocity of light.

The crystal structure of antimony is rhombohedral. If we assume for the Fermi surface of antimony the three-ellipsoid model of Shoenberg,[11] we have for the principal ellipsoid:

$$2m_0E_F=\alpha_{11}p_x^2+\alpha_{22}p_y^2+\alpha_{33}p_z^2+2\alpha_{23}p_yp_z, \tag{2}$$

and

$$2m_0E_F=\frac{\alpha_{11}+3\alpha_{22}}{4}p_x^2+\frac{\alpha_{22}+3\alpha_{11}}{4}p_y^2+\alpha_{33}p_z^2 +\alpha_{33}p_yp_z\pm\sqrt{3}p_xp_z\pm\sqrt{3}(\alpha_{22}-\alpha_{11})p_xp_y, \tag{3}$$

for the principal ellipsoid rotated $\pm120°$ about the z axis, where z is the threefold axis, x the binary, and y the bisectrix. This is the most general ellipsoidal surface allowed by symmetry.

The periods of the dHvA oscillations derived using Eqs. (1), (2), and (3) are, with H in z-y plane, $q\|x$, and θ from z axis:

$$\Delta\left(\frac{1}{H}\right)_1=\frac{e\hbar}{cm_0E_F}[\alpha_{11}\alpha_{22}\cos^2\theta+\alpha_{11}\alpha_{33}\sin^2\theta -2\alpha_{33}\alpha_{11}\sin\theta\cos\theta]^{1/2}, \tag{4}$$

$$\Delta\left(\frac{1}{H}\right)_{2,3}=\frac{e\hbar}{cm_0E_F}\left[\alpha_{11}\alpha_{22}\cos^2\theta+\alpha_{23}\alpha_{11}\sin\theta\cos\theta +\frac{3(\alpha_{22}\alpha_{33}-\alpha_{23}^2)+\alpha_{33}\alpha_{11}}{4}\sin^2\theta\right]^{1/2}. \tag{5}$$

with H in z-x plane, $q\|y$, and θ from z axis:

---

* Submitted as a thesis in partial fulfillment of the requirements for the degree of Doctor of Philosophy at the University of Chicago.

† The work was supported in part by a grant from the National Science Foundation to the University of Chicago for research in solid-state properties of bismuth, antimony, and arsenic.

‡ Raytheon pre-doctoral fellow.
§ Present address: Argonne National Laboratory; Argonne, Illinois.

[1] B. W. Roberts, Phys. Rev. Letters **6**, 453 (1961).
[2] M. H. Cohen, M. J. Harrison, and W. A. Harrison, Phys. Rev. **117**, 937 (1960).
[3] H. E. Bömmel, Phys. Rev. **100**, 758 (1955).
[4] A. B. Pippard, Phil. Mag. **2**, 1147 (1957).
[5] R. W. Morse, H. V. Bohm, and J. D. Gavenda, Phys. Rev. **109**, 1394 (1958).
[6] D. Reneker, Phys. Rev. **115**, 303 (1959).
[7] D. Gibbons, Phil. Mag. **6**, 445 (1961).
[8] Y. Eckstein, preceding paper [Phys. Rev. **129**, 12 (1963)].
[9] H. Stolz (private communication).
[10] L. Onsager, Phil. Mag. **43**, 1006 (1952).
[11] D. Shoenberg, Proc. Roy. Soc. (London) **345**, 1 (1952).

$$\Delta\left(\frac{1}{H}\right)_1=\frac{e\hbar}{cm_0E_F}[\alpha_{11}\alpha_{22}\cos^2\theta+(\alpha_{22}\alpha_{33}-\alpha_{23}^2)\sin^2\theta]^{1/2}, \quad (6)$$

$$\Delta\left(\frac{1}{H}\right)_{2,3}=\frac{e\hbar}{cm_0E_F}\left[\alpha_{11}\alpha_{22}\cos^2\theta\pm\sqrt{3}\alpha_{23}\alpha_{11}\sin\theta\cos\theta+\frac{(\alpha_{22}\alpha_{33}-\alpha_{23}^2)+3\alpha_{11}\alpha_{33}}{4}\sin^2\theta\right]^{1/2}. \quad (7)$$

with H in x-y plane, $q\|z$, and θ from x axis:

$$\Delta\left(\frac{1}{H}\right)_1=\frac{e\hbar}{cm_0E_F}[(\alpha_{22}\alpha_{33}-\alpha_{23}^2)\cos^2\theta+\alpha_{11}\alpha_{33}\sin^2\theta]^{1/2}, \quad (8)$$

$$\Delta\left(\frac{1}{H}\right)_{2,3}=\frac{e\hbar}{cm_0E_F}\left[\frac{(\alpha_{22}\alpha_{33}-\alpha_{23}^2)}{4}\cos^2\theta+\frac{\alpha_{33}\alpha_{11}+3(\alpha_{22}\alpha_{33}-\alpha_{23}^2)}{4}\sin^2\theta\right]^{1/2}. \quad (9)$$

The subscript 1 refers to the principal ellipsoid and 2, 3 to the nonprincipal ellipsoids. The components of the reciprocal mass tensor α_{ij} are related to the mass tensor m_{ij} of Shoenberg by the relations

$$m_{11}=\frac{m_0}{\alpha_{11}}, \quad m_{22}=\frac{\alpha_{33}m_0}{\alpha_{22}\alpha_{33}-\alpha_{23}^2},$$

$$m_{33}=\frac{\alpha_{22}m_0}{\alpha_{22}\alpha_{33}-\alpha_{23}^2}, \quad m_{23}=-\frac{\alpha_{23}m_0}{\alpha_{22}\alpha_{33}-\alpha_{23}^2}.$$

EXPERIMENT

Antimony from the Ohio Semiconductor Company, of quoted impurity content less than one part per million, was formed into single crystals by the Czochralski method. The crystals were oriented to within 1° by Laue back-diffraction x rays, and cut into suitable samples approximately 1 cm in thickness and 1 cm² in area. The first samples were cut with an acid string saw, using equal mixtures of concentrated HF and concentrated HNO_3. The surfaces were then ground parallel to better than 10^{-2} mm over the surface of the crystal with an automatic abrasive lapper. This method of lapping was found to do considerable damage to the crystals and so was discarded. On later samples a spark cutter and planer were used and this improved the mean free path by a factor of 10. The mean free path at 1.2°K obtained from observing the number of oscillations in geometric resonance was approximately 1 mm which was significantly longer than at 4.2°K. All data presented here were taken on the later crystals at 1.2°K.

Quartz x-cut transducers of fundamental frequency 12 Mc/sec, and gold plated in a manner described by Huntington[12] were bonded to both sides of the sample.

[12] H. B. Huntington, Phys. Rev. 72, 321 (1947).

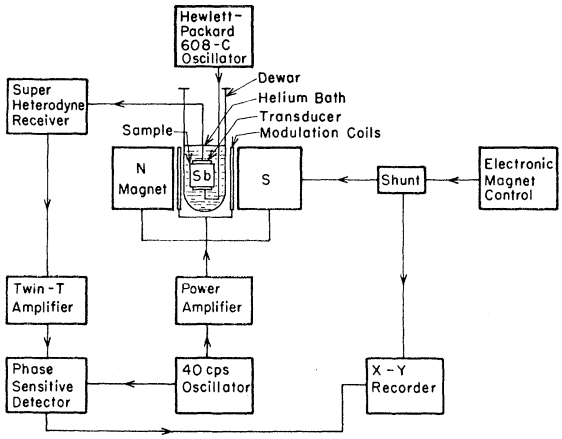

FIG. 1. Block diagram of experiment.

With this method of plating, electrical connections proved no problem. The bond used was Dow Corning No. 200 silicone fluid of viscosity 2.5×10^6 centistokes. This substance is still plastic at helium temperatures. Of the many bonds tried, this one was found to be the only suitable one.

A standard cryogenic arrangement with a dual coaxial line sample holder was used, and the temperature of the helium bath was controlled by pumping. The coaxial lines were terminated with the transducers and no attempt at impedance matching was made. An electronically controlled magnet of maximum field 9200 G was used. Calibration of the magnet was done with nuclear magnetic resonance. The stability of the magnet was one part in a thousand.

Pulsed 12-Mc/sec rf power from an Arenberg pulsed oscillator was applied to the first transducer, propagated as an acoustic wave through the sample, received by the second transducer at the opposite face of the sample, detected by a low-noise superheterodyne receiver, and displayed on an oscilloscope. With this arrangement we could make certain that the electronics was working and that both transducer bonds were satisfactory. For the actual measurements we used the less direct though more sensitive derivative method of Reneker because of the small amplitude of the oscillations. A block diagram is shown in Fig. 1. In this scheme, continuous 12-Mc/sec power from a Hewlett-Packard 608C oscillator replaced the pulsed oscillator. Modulation coils attached to the magnet and driven by a power amplifier, which was in turn driven by a 40-cps oscillator, caused an oscillating change in attenuation which was demodulated by a phase-sensitive detector. A narrow bandwidth is first achieved by a Twin-T amplifier of bandwidth $\Delta f/f=1/40$. A phase-sensitive detector synchronously rectifies the 40-cps signal. The resulting dc signal can then be integrated to further reduce noise fluctuations. This further reduces the bandwidth down to a value as small as 1/25 cps in our unit. The rms Johnson noise is given by $E^2=4kTR\Delta f$ so that the reduction of the necessary

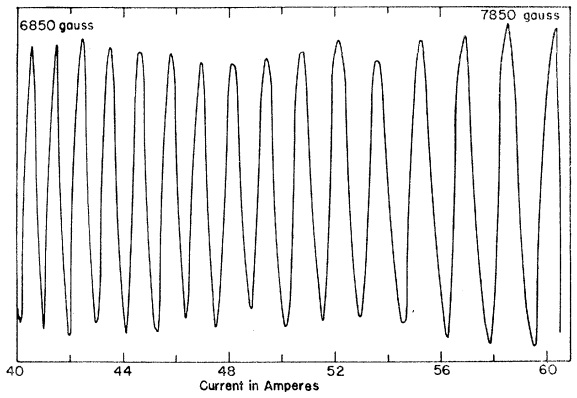

FIG. 2. A typical set of oscillations.

2-Mc/sec bandwidth of the pulsed method to the 1/25 cps of the continuous method increases the signal-to-noise ratio by more than 1000. The field was increased slowly enough to avoid integration time errors. The output of the phase-sensitive detector was applied to the y axis of a brown x-y recorder, while the output of a calibrated shunt recorded the current in the magnet on the x axis. Since the dHvA oscillations in antimony are quite close together for the fields used in this experiment, a scheme was used to magnify any portion of the x axis by subtracting a known dc voltage and using a high-sensitivity shunt. Since the attenuation of the sound wave is given by $A=A_0e^{-\alpha L}$, a small change in the magnetic field H causes a change $\Delta\alpha=(d\alpha/dH)_{H=0}\Delta H$ and the attenuation to first order becomes $\Delta A/\Delta H=A_0e^{-\alpha L}(d\alpha/dH)_{H=0}$. This derivative action reduces the amplitude of oscillations at high fields by a factor $1/H^2$ and emphasizes more rapid oscillations. We see that the derivative technique is sensitive to only a narrow range of periods since long periods are suppressed by the action of the derivative and one would expect short periods to be damped by an exponential factor containing the effective mass.

DISCUSSION

A typical set of oscillations is shown in Fig. 2 while a plot of the oscillation number n vs $1/H$ from which the period was obtained is shown in Fig. 3. In a typical sample, oscillations were seen above 4000 G. The amplitude of the oscillations was larger at 1.2°K than it was at 4.2°K. Plots of the observed periods vs angle are shown in Figs. 4–6 together with the data taken by Shoenberg. Oscillations for $q\|x$ were typically much weaker in amplitude. Comparison of the values of the observed periods in the x-y plane to those of Shoenberg showed that in this plane the carriers observed are those he analyzed; in the other two planes evidence of another carrier is observed in addition to the carriers of Shoenberg which are now seen only over a limited range of angles. Since our data agree with Shoenberg wherever his carriers are observable, we may conclude that the oscillations we observe are of the dHvA type.

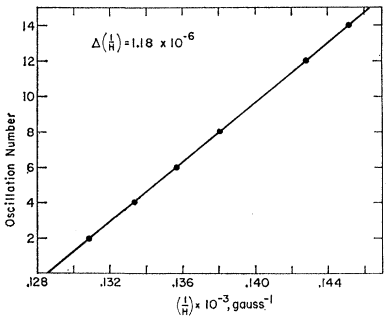

FIG. 3. The $1/H$ plot for the previous oscillations.

Equations (4)–(9) can be rewritten in the form

$$[\Delta(1/H)]^2=-A\cos(2\theta+\phi)+B=e^2c^2/h^2\mathfrak{A}^2. \quad (10)$$

A least-squares fit of our new data to Eq. (10) was made for the dominant periods in each of the three planes with the following results:

	$A\times10^{12}$	$B\times10^{12}$	ϕ
x-y plane; $q\|x$	1.09±4%	1.06±4%	8°±2°
x-y plane; $q\|z$	1.07±4%	1.04±4%	···
x-z plane; $q\|y$	0.83±4%	0.81±4%	0°

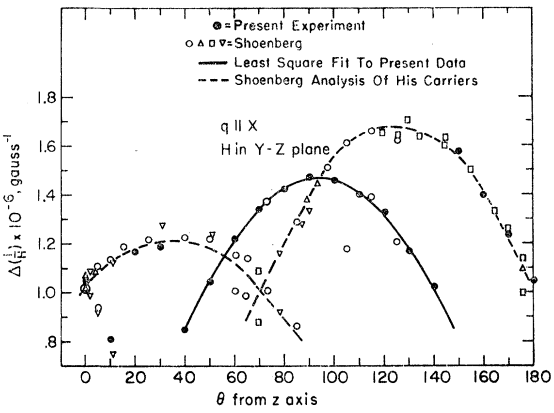

FIG. 4. Observed periods for H in the y-z plane and $q\|x$.

$A<B$ is the equation of an ellipse, $A=B$ is a parabola, and $A>B$ is a hyperbola. It will be noticed that in every case the least-squares fit is slightly hyperbolic. This behavior was also observed by Eckstein. Cohen[13] has pointed out that such nonellipsoidal behavior is to be expected for small band gaps and large anisotropy. There are not enough data to determine the extra parameters necessary to fit the surfaces he described. All analysis was carried out using an ellipsoidal model.

Since A is equal to B within experimental error we take only the sum $A+B$ in this discussion. We have with the tilt angle ϕ, three experimental results for the new carriers. Since this is insufficient to determine α_{11}, α_{22}, α_{33}, and α_{23} we will combine the present data with those of Eckstein. The combined data are shown in

[13] M. H. Cohen, Phys. Rev. **121**, 387 (1961).

TABLE I. Summary of experimental data.

Observed area in momentum space of the x-z plane ($q\|\|x$)	$(0.722\pm0.14)\times10^{-40}$ cgs
Observed area in momentum space of the y-z plane ($q\|\|y$)	$(0.828\pm0.17)\times10^{-40}$ cgs
Observed angle of minimum area for H in the y-z plane ($q\|\|x$)	$4°\pm1°$
Observed maximum projected momentum of x-z plane on the z axis ($q\|\|x$)	$(0.350\pm1.7)\times10^{-20}$ cgs
Observed maximum projected momentum of y-z plane on the z axis ($q\|\|y$)	$(0.430\pm2.2)\times10^{-20}$ cgs
Observed angle of minimum momentum for H in the y-z plane ($q\|\|x$)	$3°\pm1°$

Table I. To compute the elements of the reciprocal mass tensor, we have to know which ellipsoid is making the dominant contribution to the period. Two possibilities were found that fit the data. The best combination found was to assume Eckstein was observing the non-principal ellipsoid for H in the y-z plane and the principal ellipsoid for H in the x-z plane while the present experiment observed the principal ellipsoid for H in the y-z and x-z planes.

The second possibility was to assume that with the field in the y-z plane, and we both observed the non-principal ellipsoid while for the field in the x-z plane, we both observed the principal ellipsoid. If for the first possibility we use Eqs. (4) and (6) together with Eqs. (1b), (2a), and the tilt angle of Eckstein, then the data of Table I take the form:

Present experiment

(a) $\alpha_{11}\alpha_{33}=(0.626\pm0.025)\times10^{28}E_F^2$,

(b) $\alpha_{22}\alpha_{33}-\alpha_{23}^2=(0.477\pm0.019)\times10^{28}E_F^2$,

(c) $2\alpha_{23}/(\alpha_{33}-\alpha_{22})=0.140\pm0.04$;

Eckstein

(d) $\alpha_{33}-3\alpha_{23}^2/(\alpha_{11}+3\alpha_{22})=(1.485\pm0.059)\times10^{14}E_F$,

(e) $(\alpha_{22}\alpha_{33}-\alpha_{23}^2)/\alpha_{22}=(0.984\pm0.039)\times10^{14}E_F$,

(f) $4\alpha_{23}\alpha_{11}/[3(\alpha_{22}\alpha_{33}-\alpha_{23}^2)+\alpha_{33}\alpha_{11}-4\alpha_{11}\alpha_{22}]=1.05\pm0.04$.

For the second possibility we use Eqs. (5) and (6) together with Eqs. (1b) and (2a) and the tilt angle of Eckstein and get:

Present experiment

(a) $[3(\alpha_{22}\alpha_{33}-\alpha_{23}^2)+\alpha_{33}\alpha_{11}]/4=(0.626\pm0.025)\times10^{28}E_F^2$,

(b) $\alpha_{22}\alpha_{33}-\alpha_{23}^2=(0.477\pm0.019)\times10^{28}E_F^2$,

Eckstein

(d) $\alpha_{33}-3\alpha_{23}^2/(\alpha_{11}+3\alpha_{22})=(1.485\pm0.059)\times10^{14}E_F$,

(e) $(\alpha_{22}\alpha_{33}-\alpha_{23}^2)/\alpha_{22}=(0.984\pm0.039)\times10^{14}E_F$.

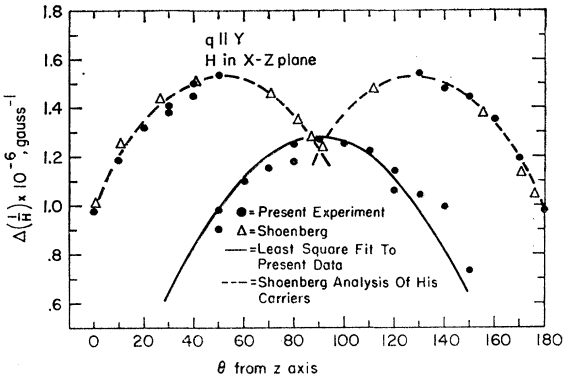

FIG. 5. Observed periods for H in the x-z plane and $q\|\|y$.

Present experiment

(c) $4\alpha_{23}\alpha_{11}/[3(\alpha_{22}\alpha_{33}-\alpha_{23}^2)+\alpha_{33}\alpha_{11}-4\alpha_{11}\alpha_{22}]=(0.14\pm0.04)$,

Eckstein

(f) $4\alpha_{23}\alpha_{11}/[3(\alpha_{22}\alpha_{33}-\alpha_{23}^2)+\alpha_{33}\alpha_{11}-4\alpha_{11}\alpha_{22}]=(0.105\pm0.04)$.

Possible values of the elements of the reciprocal mass tensor derived from these two sets of expressions are shown in Table II.

TABLE II. Values of α_{ij} for new carriers derived from experimental data.

Possibility 1	Possibility 2
$\alpha_{11}=0.0067\times10^{14}E_F$	$\alpha_{11}=0.0128\times10^{14}E_F$
$\alpha_{22}=0.4506\times10^{14}E_F$	$\alpha_{22}=0.562\times10^{14}E_F$
$\alpha_{33}=95.8\times10^{14}E_F$	$\alpha_{33}=84.2\times10^{14}E_F$
$\alpha_{23}=6.60\times10^{14}E_F$	$\alpha_{23}=6.84\times10^{14}E_F$

The fit is better for the first possibility but the anisotropy is greater. Considerations as to which periods should have been observed in a derivative technique lead us to discard the first possibility. It will be noticed that the anisotropy is very large. Introduction of non-ellipsoidal model would probably reduce this anisotropy. It will be noticed that in every case the periods of the new carriers disappear when the field is perpendicular to cross sections of the Fermi surface of large area. To investigate these portions of the surface, high fields will be required. A principal axis transformation on the

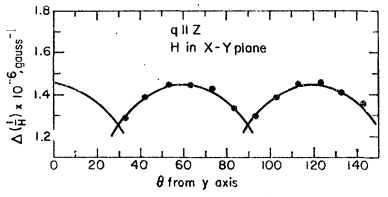

FIG. 6. Observed periods for H in the x-y plane and $q\|\|z$.

reciprocal mass tensors reveals that the Fermi surface is disk shaped.

CONCLUSIONS

An ellipsoidal fit has been made to the Fermi surface of the new carriers. The fit is in all likelihood a distortion of the true surface. Analysis beyond the data given in Table I should await high-field dHvA measurements.

ACKNOWLEDGMENTS

The author wishes to express his gratitude to his sponsor, Professor A. W. Lawson, for suggesting the problem and for continued support and encouragement; also to Professor M. H. Cohen for helpful discussions. He also wishes to thank Dr. M. G. Priestley for reading the manuscript.

PHYSICAL REVIEW VOLUME 129, NUMBER 1 1 JANUARY 1963

Relation between Elastic Constants and Second- and Third-Order Force Constants for Face-Centered and Body-Centered Cubic Lattices

ROSEMARY A. COLDWELL-HORSFALL*†
H. H. Wills Physics Laboratory, Bristol, England
(Received 27 July 1962)

The symmetry properties of a lattice are used to relate the second and third order force constants to the elastic constants of the lattice and to ascertain the number of independent force constants. Explicit relations are obtained for a face-centered cubic lattice with nearest neighbor interaction between atoms, and for a body-centered cubic lattice with nearest and next-nearest neighbor interactions. Corresponding relations are obtained for central forces in these two lattices.

I. INTRODUCTION

THE renewal of interest in the anharmonic properties of solids during the last few years draws attention to the problem of determining the force constants which appear in the theory of lattice dynamics. For the case of central forces, the interatomic potential can be characterized by two parameters, the well depth and the equilibrium interatomic separation. These are determined by measurement of the sublimation energy of the crystal and of its lattice spacing, respectively. The force constants are then obtained directly by differentiation of the interatomic potential with respect to the atomic separation. However, it has been shown[1] that a potential, such as the Mie–Lennard-Jones $(m,6)$ potential, does not give very good agreement with the experimental data available for the inert gas solids for any of the values $m=10$, 11, 12, 13, 14. The parameter m is a measure of the steepness of the repulsive part of the potential well. It has been suggested[1] that a third term might reasonably be added to the Mie–Lennard-Jones potential. If this term represents the dipole-quadrupole contribution to the van der Waals energy, the interatomic potential will have the form

$$\phi(r)=Ar^{-m}+Br^{-8}+Cr^{-6},$$

where r is the interatomic separation. Since there are now three parameters apart from m in the expression for $\phi(r)$, it is necessary to have experimental data in addition to that mentioned above in order to determine the third parameter. Though difficult to obtain in the case of the inert gas solids, the elastic constants are an obvious choice for this purpose. Therefore, it seems worthwhile to set forth here relations between the elastic constants and the force constants. Furthermore, in obtaining these relations we ascertain the number of independent force constants which arise in the lattice model under consideration.[2] This information is important when one is considering the possibility of extending a nearest neighbor, central force theory to noncentral forces, and further neighbors. It must be emphasized that the force constants are derivatives of the potential energy evaluated at the minimum of the potential energy, and that in the relations which we obtain, the elastic constants are also appropriate to the configuration which corresponds to the minimum of the potential energy. Since dynamic effects are excluded, the relations which we obtain correspond to elastic constants at the absolute zero of temperature in the approximation for which there is no zero-point motion. In order to determine these elastic constants from the experimental data, the zero-point energy of the lattice must be taken into account and the temperature dependence of the elastic constants must be determined. This problem will not be considered here.

* NATO Research Fellow.
† Permanent address: Department of Physics, The University, Sheffield, England.
[1] G. K. Horton and J. W. Leech (to be published).

[2] The independent force constants for fcc and bcc lattices with nearest neighbor interaction have also been obtained by G. Leibfried and W. Ludwig in *Solid State Physics*, edited by F. Seitz and D. Turnbull (Academic Press Inc., New York, 1961), Vol. 12.